

Discovery and Characterization of the TB Drug Lead Ecumicin

Wei Gao,^{†,‡} Jin-Yong Kim,^{§,||} Shao-Nong Chen,[†] Sang-Hyun Cho,[‡] Jongkeun Choi,[⊥] Birgit U. Jaki,^{†,‡} Ying-Yu Jin,^{||} David C. Lankin,[†] Ji-Ean Lee,^{||} Sun-Young Lee,^{§,||} James B. McAlpine,^{†,‡} José G. Napolitano,[†] Scott G. Franzblau,[‡] Joo-Won Suh,^{§,||,*} Guido F. Pauli^{†,‡,*}

[†]Department of Medicinal Chemistry and Pharmacognosy, College of Pharmacy, University of Illinois at Chicago, Chicago, IL 60612, U.S.A. [‡]Institute for Tuberculosis Research, College of Pharmacy, University of Illinois at Chicago, 833 S. Wood St. Chicago, Illinois 60612 U.S.A. [§]Division of Bioscience and Bioinformatics, College of Natural Science, Myongji University, Cheoin-gu, Yongin, Gyeonggi-Do 449-728, South Korea. ^{||}Center for Nutraceutical and Pharmaceutical Materials, Myongji University, Cheoin-gu, Yongin, Gyeonggi-Do 449-728, South Korea. [⊥] Department of Cosmetic Science, Chungwoon University, Hongseong Chungnam 350-701, South Korea.

Supporting Information

Table of Contents

I. General Procedures	S2
II. Supplementary Results	S3
III. IR, UV and CD Spectra of Ecumicin (1)	S8
IV. NMR Spectra and Assignments of Ecumicin (1)	S11
V. MS spectra and assignments.....	S22
VI. X-ray crystallography data.....	S24

I. General Procedures

1D and 2D NMR spectra were obtained on a Bruker DPX 400 MHz with a 5 mm ATM CPTCI Z-gradient probe, Bruker Avance 600 MHz NMR spectrometer with a 5 mm CPTXI Z-gradient probe and a Bruker Avance II 900MHz NMR spectrometer with a 5 mm ATM CPTCI Z-gradient probe. ^1H and ^{13}C NMR chemical shifts were referenced to the methanol- d_4 solvent signals (δ_{H} 3.310 and δ_{C} 49.00, respectively). A mixing time of 60 ms was set for the TOCSY experiment and 200 ms for the ROESY experiment. The HMBC spectra were recorded with the $^3J_{\text{C-H}}$ set to 8 Hz, and the HSQC spectra were collected with the $^1J_{\text{C-H}}$ set to 140 Hz. High-resolution ESI mass spectra were obtained using a Shimadzu IT-TOF LC mass spectrometer. Tandem mass analysis was performed using a Micromass Q-TOF LC mass spectrometer.

Marfey's analysis

The analysis was carried out as described.¹ 0.3 mg peptide was mixed with 0.5 ml 6N HCl solution. The mixture was heated at 110°C for 16 hours, and the resultant solution was dried under vacuum. 100 μg hydrolyte, L-valine (Sigma-Aldrich), D-valine (Sigma-Aldrich), N-methyl-L-valine (Sigma-Aldrich) was mixed with 20 μL 1M NaHCO_3 and 10 μL 10% L-FDAA (Sigma-Aldrich) in acetone. The solution was heated to 80°C for 3 min, and then cooled down to room temperature. 20 μL 1M HCl was then added to neutralize the solution. The reprivatized sample was then diluted to approximately 1 $\mu\text{g}/\text{mL}$ with acetonitrile. 5 μL of diluted sample was injected into a RP-C18 column (Xterra® MS C18 3.5 μm 2.1x150 mm), and a bi-phase gradient method starting from 0.1% FA acetonitrile solution: 0.1% FA water solution = 20:80 (v/v) to 50:50 (v/v) in 30 min was applied. MS detector was set to scan mode with m/z from 200 to 600, and SIM mode with m/z of 370, and 384.

References

- (1) Bhushan, R.; Bruckner, H. *J. Chromatogr. B*, **2011**, 879, 3148.

II. Supplementary Results

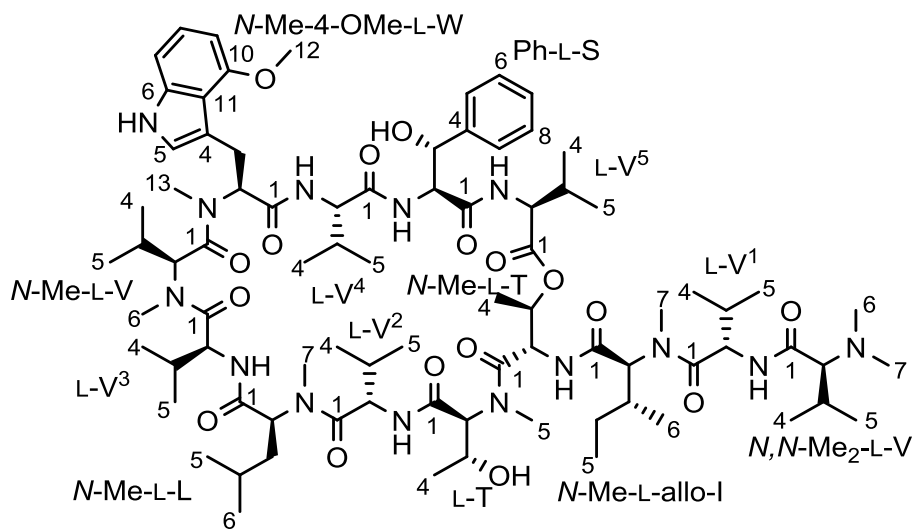
Purity of Ecumicin (1) in Sample H14 Assessed by 100% qHNMR

The ^1H NMR spectrum of fraction H14 (900 MHz, CD_3OD , Figure S6) was acquired under quantitative conditions [90 degree excitation pulse (10.25 μs , acquisition time 4.0 s; relaxation delay 60.0 s] using a Bruker Avance II 900 instrument. Processing, used zero filling (2x), Lorentzian-Gaussian apodization (LB=-0.3, GB =0.05), and polynomial baseline correction.

The aromatic singlet (δ_{H} 6.698) of **1** was selected as the most pure signal, and used to quantitate **1** by applying the following integral-based 100% qHNMR method. The integral of the singlet was set to 1.000, representing the integral of one proton (1H). All other proton signals between δ_{H} 0.0 to 7.5 in the spectrum, except for the solvent signals (HOD and CHD_2OD), were integrated, and the sum of these integrals was determined to be 137.36.

A total of 125 non-exchangeable protons are present in **1**. Considering that all resonances not belonging to **1** (i.e., the impurity signals) were typical peptide resonances, and assuming that they have the same molecular weight as **1** (i.e., isomeric impurities), the purity of **1** in fraction H14 was calculated as:

$$\text{Purity} = 125 \times 1.00 / 137.36 \times 100 \% = 91 \%$$



1

Detailed 2D NMR Assignments of Ecumicin (1)

Extensive analysis of the 2D NMR spectra of **1**, particularly based on COSY, TOCSY, HSQC HMBC and semi-selective HMBC experiments (Figure S7 to Figure S12) resulted in the elucidation of 15 discrete ^1H , ^1H spin systems: *N,N*-Me₂-V, V¹, *N*-Me-I, T, *N*-Me-T, V², *N*-Me-L, V³, *N*-Me-V, *N*-Me-4-OMe-W^a, *N*-Me-4-OMe-W^b, V⁴, Ph-S^a, Ph-S^b and V⁵.

The ^{13}C and ^1H signals of aliphatic methyl groups were in very crowded regions, where 14 carbon signals representing 14 carbons were presented within a δ_{C} 0.94 window (δ_{C} 19.10 to 20.04, Figure S6). The resolution of normal HSQC and HMBC experiments was not high enough to establish connectivity for these signals, so semi-selective HMBC experiment was used. The direct H-C connectivity was built by using ^{13}C - ^1H single bond correlations extracted from semi-selective HMBC spectrum (Figure S11). Such correlations were observed with a coupling constant around 126 Hz along F2 direction. The methyl groups were connected to their spin systems respectively by using the COSY correlations between methyl proton signals and β -proton signals. Such connectivities were confirmed by ^1H , ^{13}C long range couplings between methyl proton signals and β -carbon signals, or between methyl carbon signals and β -proton signals.

Connectivity inside the *N*-Me-4-OMe-W and Ph-S units was established by using ^1H , ^{13}C long-range correlations extracted from HMBC experiment (Figure S10). Correlations were observed for *N*-Me-4-OMe-W H⁴/ *N*-Me-4-OMe-W C ^{β} , Ph-S H^{2'}/ Ph-S C ^{β} , and Ph-S H^{5'}/ Ph-S C ^{β} .

The position of the methoxyl group of *N*-Me-4-OMe-W was also determined by analyzing the HMBC spectrum. HMBC correlations were observed for *N*-Me-4-OMe-W H¹²/ *N*-Me-4-OMe-W C¹⁰, *N*-Me-4-OMe-W H⁸/ *N*-Me-4-OMe-W C⁶, *N*-Me-4-OMe-W H⁷/ *N*-Me-4-OMe-W C¹¹, *N*-Me-4-OMe-W H⁹/ *N*-Me-4-OMe-W C¹¹.

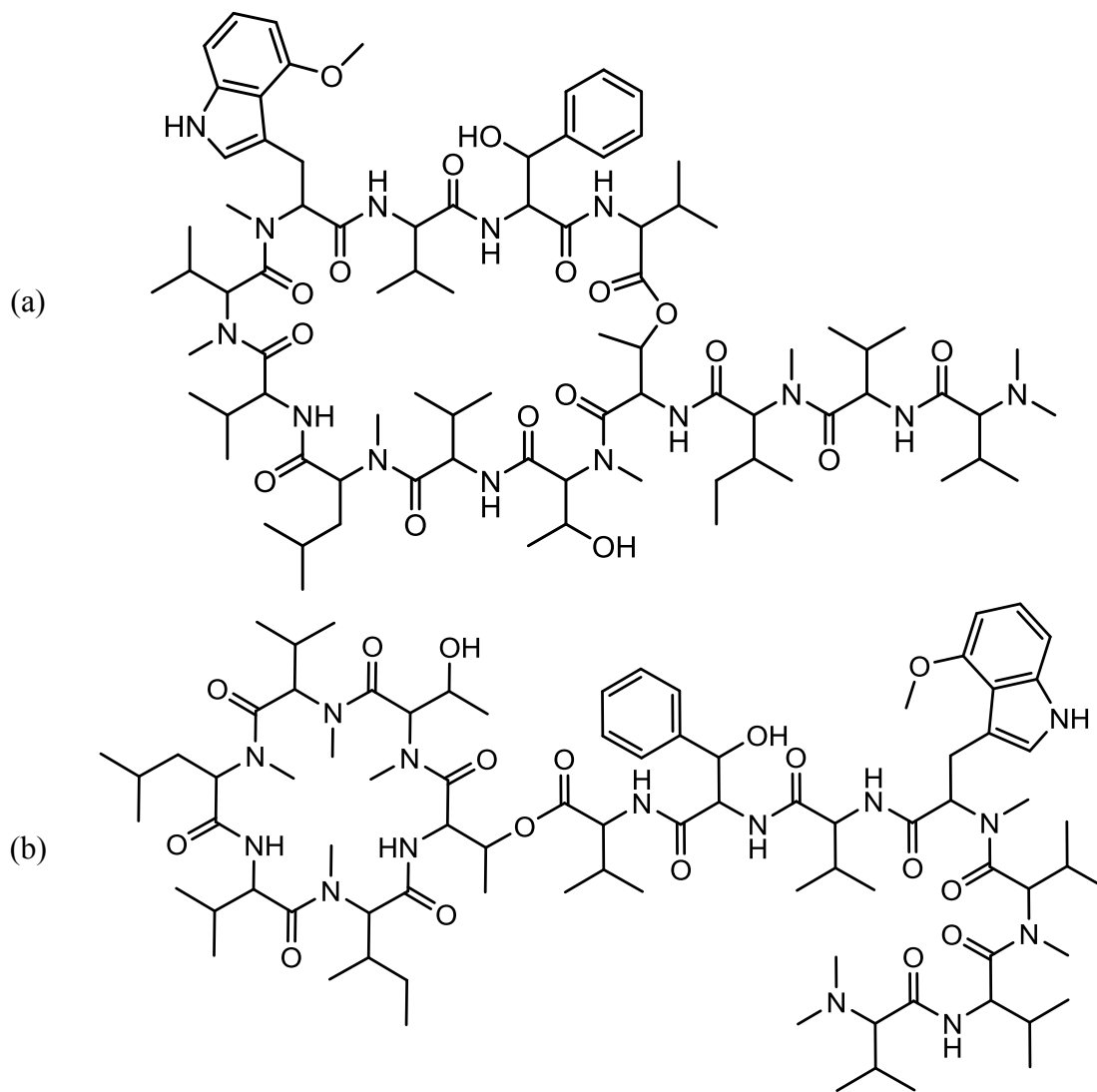
The positions of *N*-methyl and methoxyl groups were determined by analyzing HMBC correlations: (i, i) H^{NMe}/C^α (3J) and/or (i, i+1) $H^{NMe}/C^{C=O}$ (3J), where “i” indicates the location of individual amino acid residue from the N-terminus. Such correlations were observed for *N,N*-Me₂-V $H^{6(7)}/N,N$ -Me₂-V C^α , *N*-Me-I $H^7/V^1 C^{C=O}$, *N*-Me-I H^7/N -Me-I C^α , *N*-Me-T $H^5/T C^{C=O}$, *N*-Me-T H^5/N -Me-T C^α , *N*-Me-L $H^7/V^2 C^{C=O}$, *N*-Me-L H^7/N -Me-L C^α , *N*-Me-V $H^6/V^3 C^{C=O}$, *N*-Me-V H^6/N -Me-V C^α , *N*-Me-4-OMe-W H^{13}/N -Me-4-V $C^{C=O}$, *N*-Me-4-OMe-W H^{13}/N -Me-4-OMe-W C^α .

The individual amino acid residues were linked sequentially via correlations between the carbonyl carbon and the following protons: α -protons [(i, i) $H^\alpha/C^{C=O}$ (2J)], β -protons [(i, i) $H^\beta/C^{C=O}$ (3J)], neighboring α -protons [(i, i+1) $H^\alpha/C^{C=O}$ (3J)], and/or neighboring *N*-methyl protons [(i, i+1) $H^{NMe}/C^{C=O}$ (3J)]. In the formula, “i” indicates the location of individual amino acid residue from the N-terminus. Another semi-selective HMBC spectrum was acquired, to resolve the crowded carbonyl region with 13 ^{13}C signals presented in a δ_C 4.23 window (δ_C 170.91 to 175.14, Figure S6). Correlations were observed for *N,N*-Me₂-V $H^\alpha/N,N$ -Me₂-V $C^{C=O}$, *N,N*-Me₂-V $H^\beta/N,N$ -Me₂-V $C^{C=O}$, $V^1 H^\alpha/V^1 C^{C=O}$, $V^1 H^\beta/V^1 C^{C=O}$, *N*-Me-I H^α/N -Me-I $C^{C=O}$, *N*-Me-I $H^\alpha/V^1 C^{C=O}$, *N*-Me-I H^β/N -Me-I $C^{C=O}$, T $H^\alpha/T C^{C=O}$, T H^α/N -Me-I $C^{C=O}$, T $H^\beta/T C^{C=O}$, *N*-Me-T H^α/N -Me-T $C^{C=O}$, *N*-Me-T $H^\alpha/T C^{C=O}$, *N*-Me-T H^β/N -Me-T $C^{C=O}$, $V^2 H^\alpha/V^2 C^{C=O}$, $V^2 H^\alpha/N$ -Me-T $C^{C=O}$, $V^2 H^\beta/V^2 C^{C=O}$, *N*-Me-L H^α/N -Me-L $C^{C=O}$, *N*-Me-L $H^\alpha/V^2 C^{C=O}$, *N*-Me-L H^β/N -Me-L $C^{C=O}$, $V^3 H^\alpha/V^3 C^{C=O}$, $V^3 H^\beta/V^3 C^{C=O}$, *N*-Me-V H^α/N -Me-V $C^{C=O}$, *N*-Me-V $H^\alpha/V^3 C^{C=O}$, *N*-Me-V H^β/N -Me-V $C^{C=O}$, *N*-Me-4-OMe-W H^α/N -Me-4-OMe-W $C^{C=O}$, *N*-Me-4-OMe-W H^α/N -Me-V $C^{C=O}$, *N*-Me-4-OMe-W H^β/N -Me-4-OMe-W $C^{C=O}$, $V^4 H^\alpha/V^4 C^{C=O}$, $V^4 H^\alpha/N$ -Me-4-OMe-W $C^{C=O}$, $V^4 H^\beta/V^4 C^{C=O}$, Ph-S $H^\alpha/Ph-S C^{C=O}$, Ph-S $H^\alpha/V^4 C^{C=O}$, Ph-S $H^\beta/Ph-S C^{C=O}$, $V^5 H^\alpha/V^5 C^{C=O}$, $V^5 H^\alpha/Ph-S C^{C=O}$, $V^5 H^\beta/V^5 C^{C=O}$.

An HMBC correlation between T H^β and $V^5 C^{C=O}$ was observed, suggesting **1** be a cyclic depsipeptide cyclized between the C-terminal carboxyl and the hydroxyl group of the T residue. That the *N,N*-Me₂-V and *N*-Me-L units as their

carbonyl carbons resonate at the same frequency leaves two structure possibilities for **1** (Figure S1).

Figure S1. The two possible structures of **1** (a) and (b) were constructed from extensive 1D and 2D NMR analyses and could not be resolved due to the isochronicity ($\Delta\delta < 0.01$ ppm) of two carbonyl carbons.



III. IR, UV and CD Spectra of Ecumicin (1)

Figure S2. IR spectrum of 1.

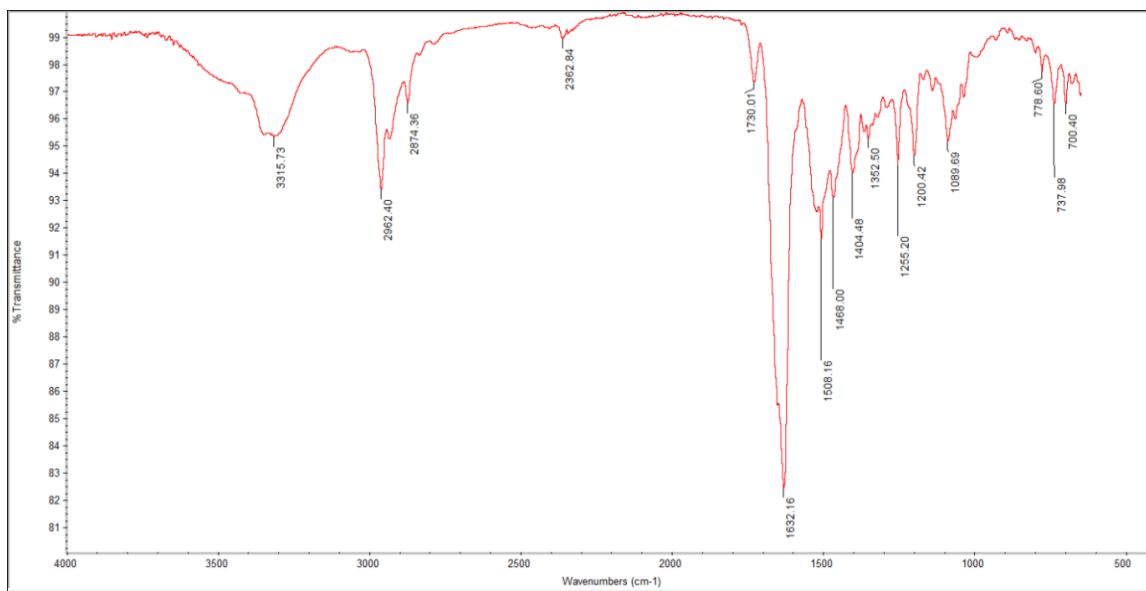
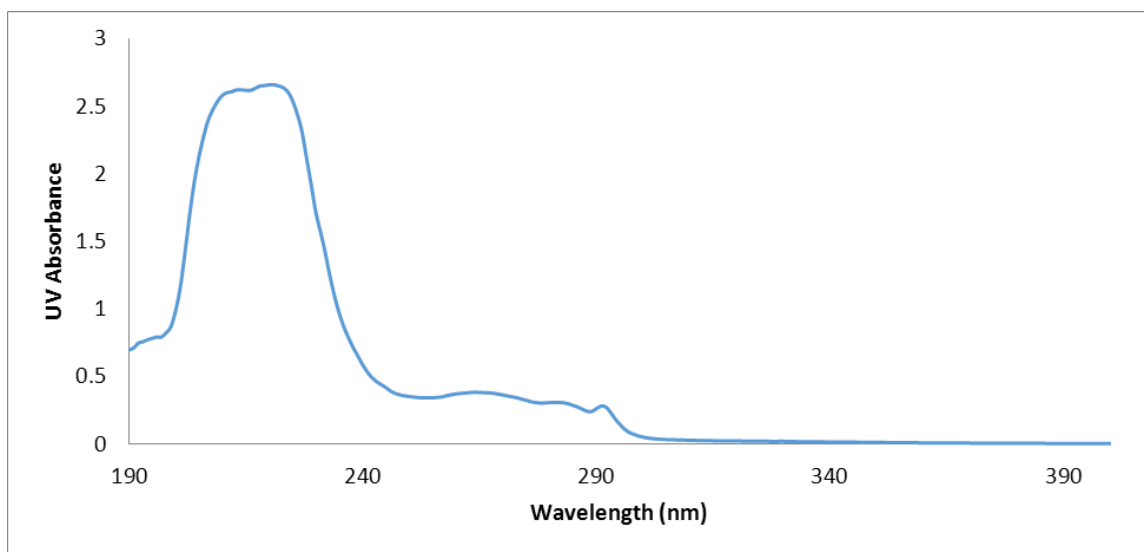


Figure S3. UV spectrum of **1**.

The spectrum was recorded with a methanol solution of **1** at 48.0 μM , in 1 cm quartz cuvette, 25°C (background subtracted).

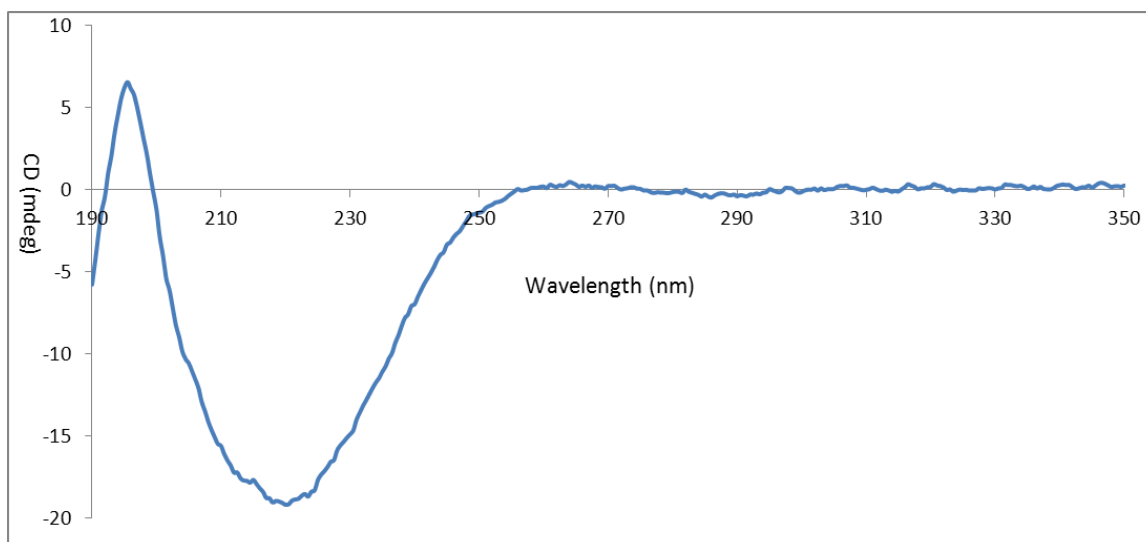
$$\epsilon = 54209 \text{ M}^{-1}\cdot\text{cm}^{-1} (211 \text{ nm})$$

$$\epsilon = 55266 \text{ M}^{-1}\cdot\text{cm}^{-1} (219 \text{ nm})$$

$$\epsilon = 7925 \text{ M}^{-1}\cdot\text{cm}^{-1} (263 \text{ nm})$$

$$\epsilon = 6465 \text{ M}^{-1}\cdot\text{cm}^{-1} (281 \text{ nm})$$

$$\epsilon = 5839 \text{ M}^{-1}\cdot\text{cm}^{-1} (291 \text{ nm})$$

Figure S4. CD spectrum of **1**.

The spectrum was recorded with an acetonitrile solution of **1** at 10 μM , in 1 cm quartz cuvette, 25°C (background subtracted), on a Jasco J 715 polarimeter.

$$[\theta]_{\text{molar}} = -1918530 \text{ deg}\cdot\text{cm}^2\cdot\text{mol}^{-1} \text{ (220 nm)}$$

$$[\theta]_{\text{molar}} = 616094 \text{ deg}\cdot\text{cm}^2\cdot\text{mol}^{-1} \text{ at 196 nm (25°C, in acetonitrile).}$$

IV. NMR Spectra and Assignments of Ecumicin (1)

The 1D NMR spectra (FIDs) of ecumicin are available online as separate Supporting Information (ZIP file). The ^1H NMR raw data of ecumicin in CD_3OD (900 MHz, Bruker Avance II 900) and the ^{13}C NMR raw data of ecumicin in CD_3OH (100 MHz, Bruker DPX-400) can be found in 1D-NMR.zip, under the folder ^1H and ^{13}C , respectively.

Figure S5. ^1H NMR Spectra of **1** in (A) CD_3OD (900 MHz, Bruker Avance II 900), and (B) CD_3OH (600MHz, Bruker Avance 600, processed with water subtraction). Expansions of the 900 MHz spectrum in regards to (C) methyl/methylene region, (D) α -proton region, (E) aromatic region, in CD_3OD , and (G) amide region in CD_3OH (600 MHz), with further expansion of the most crowded methyl region (F) in CD_3OD .

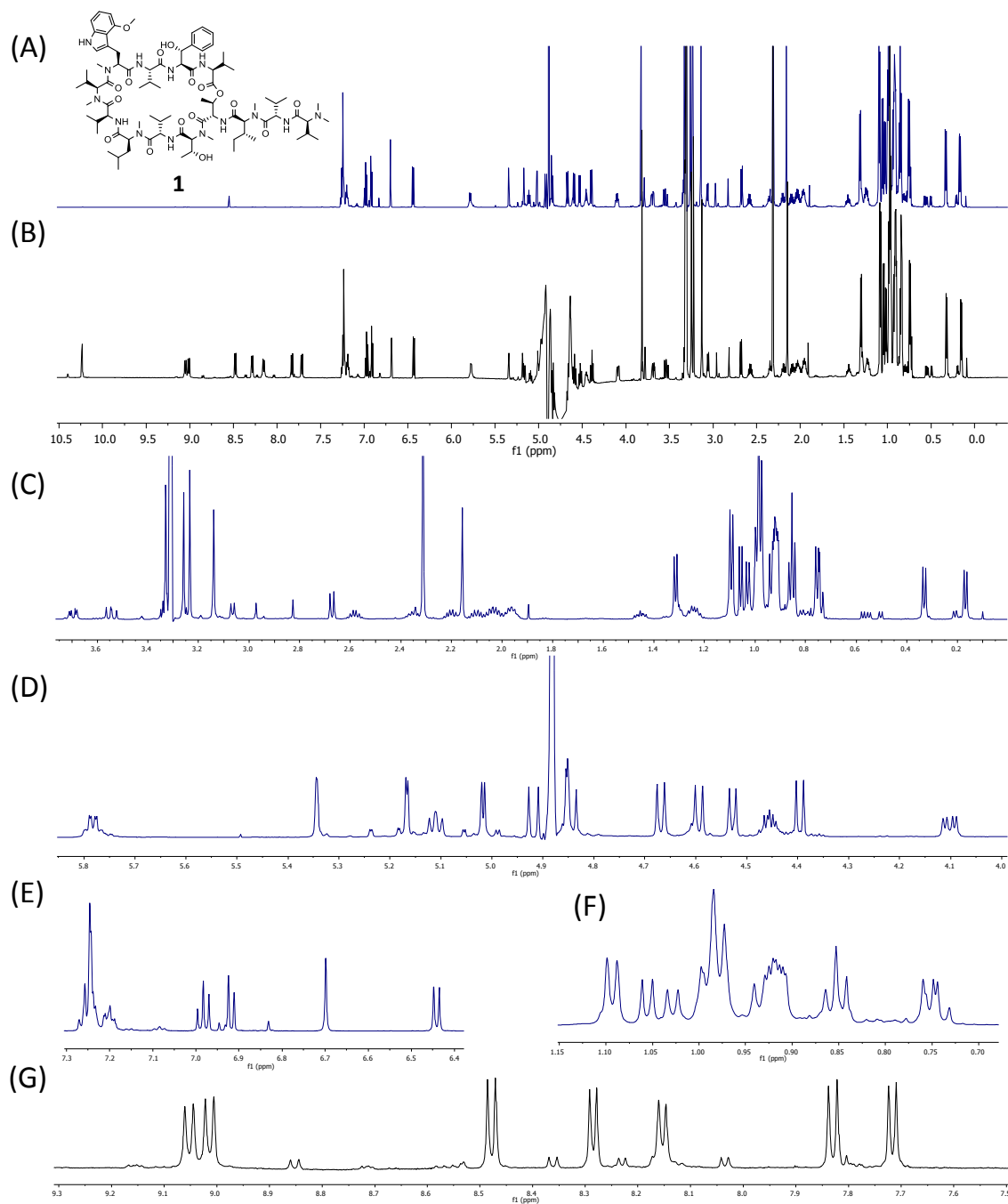


Figure S6. (A) ^{13}C and (B) DEPT-135 spectra of **1** in CD_3OH (100 MHz, Bruker DPX-400). Expansions of ^{13}C spectrum on (C) methyl/methylene region, (D) α -carbon region, (E) aromatic region, (F) carbonyl region and further expansion on the most crowded methyl region (G). (H) and (I) are expansions of DEPT-135 spectrum on the methylene carbons.

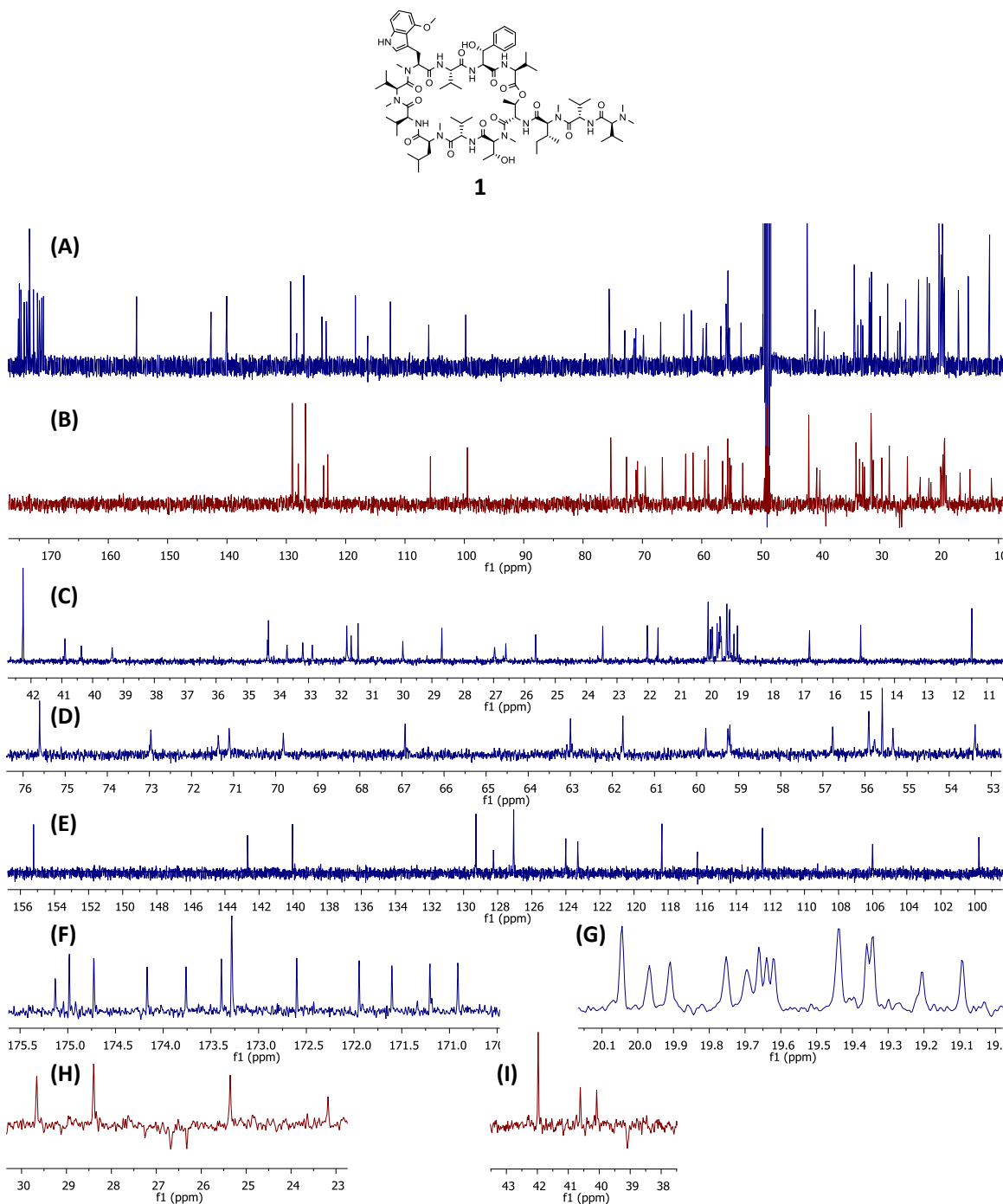


Figure S7. COSY spectrum of **1** in CD₃OD (600 MHz, Bruker Avance 600). The spectrum was acquired at (TD) 2048×256, in 32 scans. It was zero filled to 4k×4k, without linear prediction. The spectrum was not symmetrized during processing.

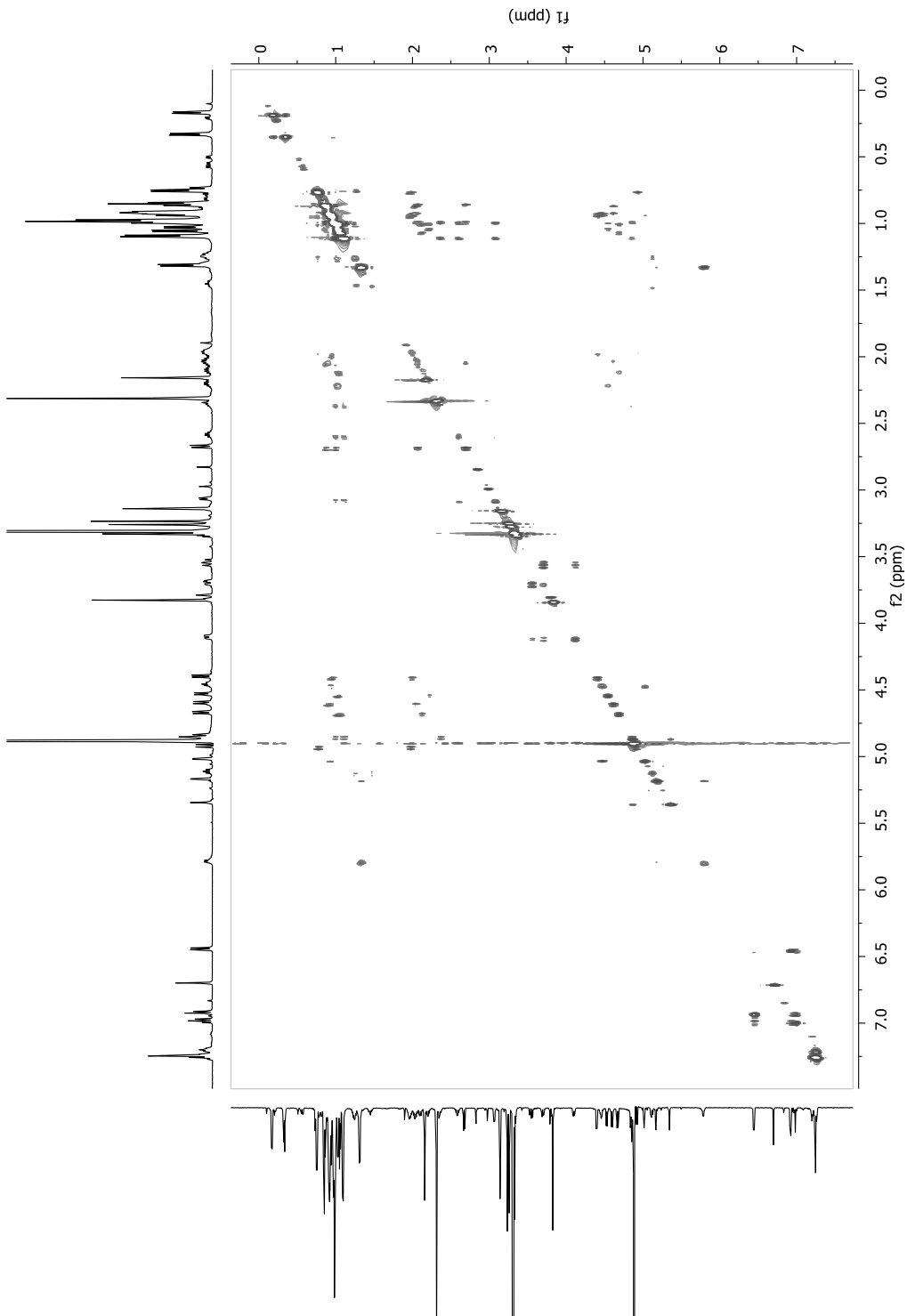


Figure S8. TOCSY spectrum of **1** in CD₃OD (600MHz, Bruker Avance 600). The spectrum was acquired at (TD) 4096x256, in 16 scans. It was zero filled to 4kx4k, without linear prediction. The spectrum was not symmetrized during processing.

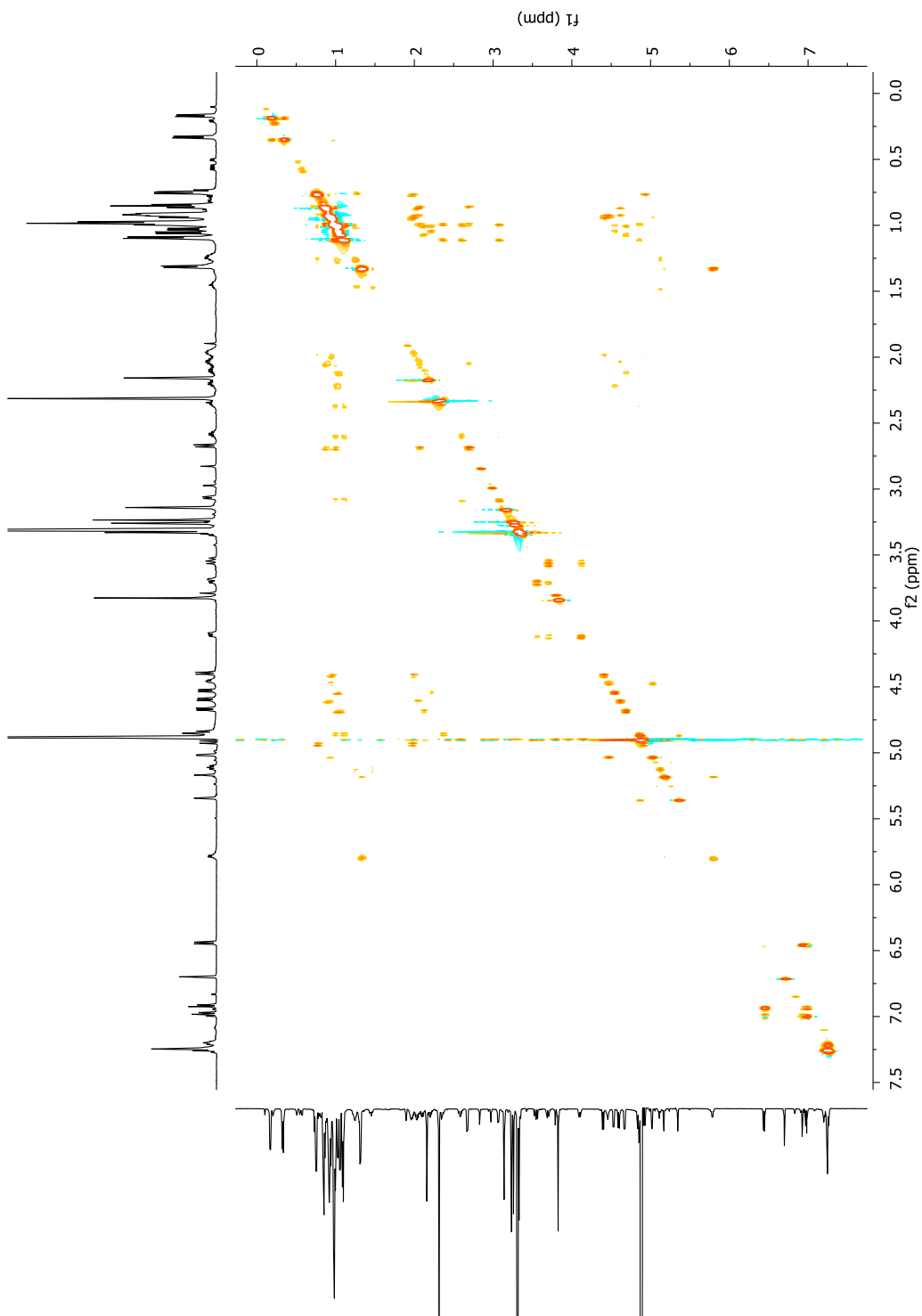


Figure S9. HSQC spectrum of **1** in CD₃OD (600 MHz, Bruker Avance 600). The spectrum was acquired at (TD) 4096x256, in 32 scans. It was zero filled to 4kx4k, with forward linear prediction on f1 direction.

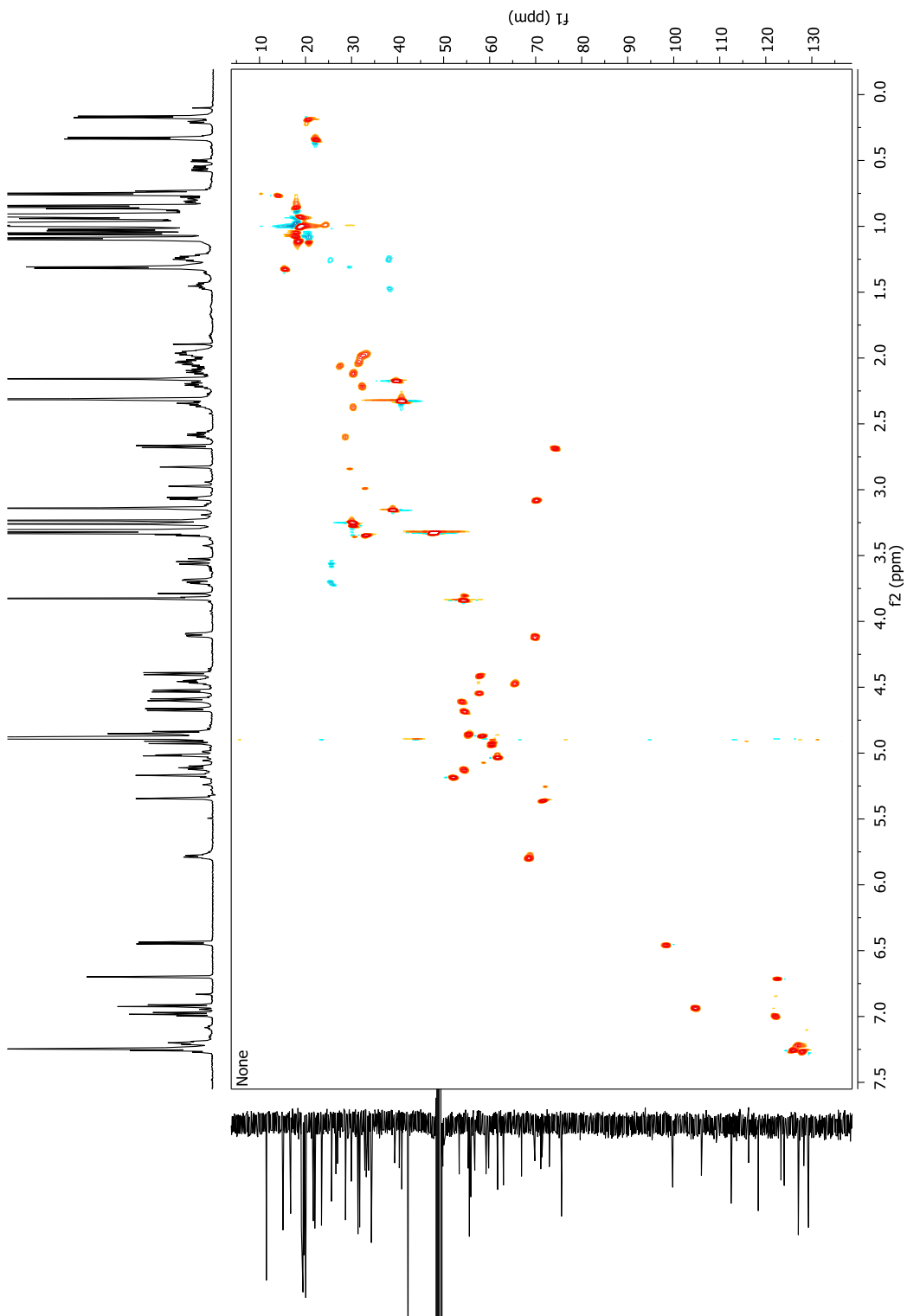


Figure S10. HMBC spectrum of **1** in CD₃OD (600 MHz, Bruker Avance 600). The spectrum was acquired at (TD) 4096x256, in 64 scans. It was zero filled to 4kx4k, with forward linear prediction on f1 direction.

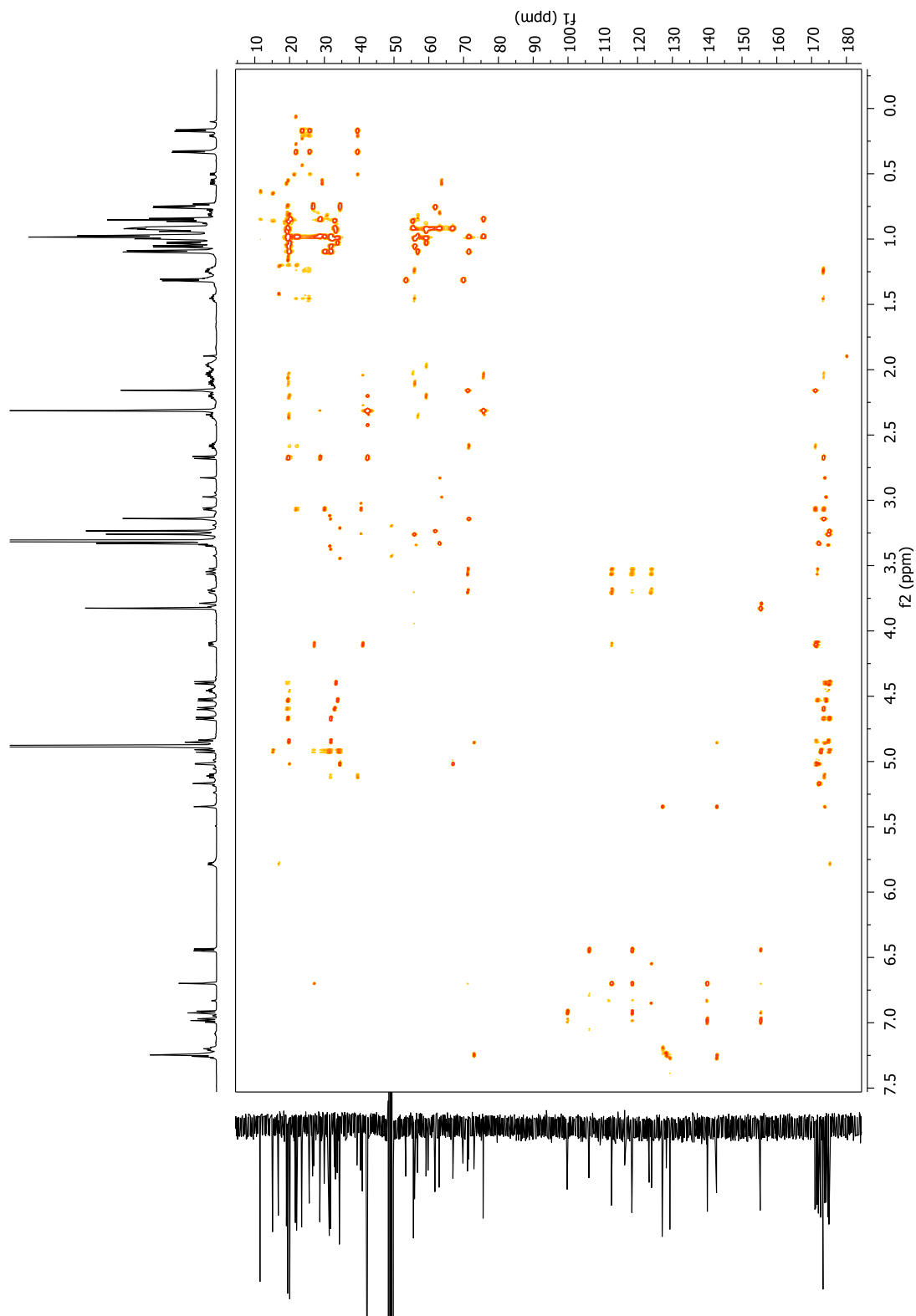


Figure S11. Semi-selective HMBC spectrum of **1** carbonyl region in CD₃OD (600 MHz, Bruker Avance 600). The spectrum was acquired at (TD) 4096x256, in 64 scans. It was zero filled to 4kx4k, with forward linear prediction on f1 direction.

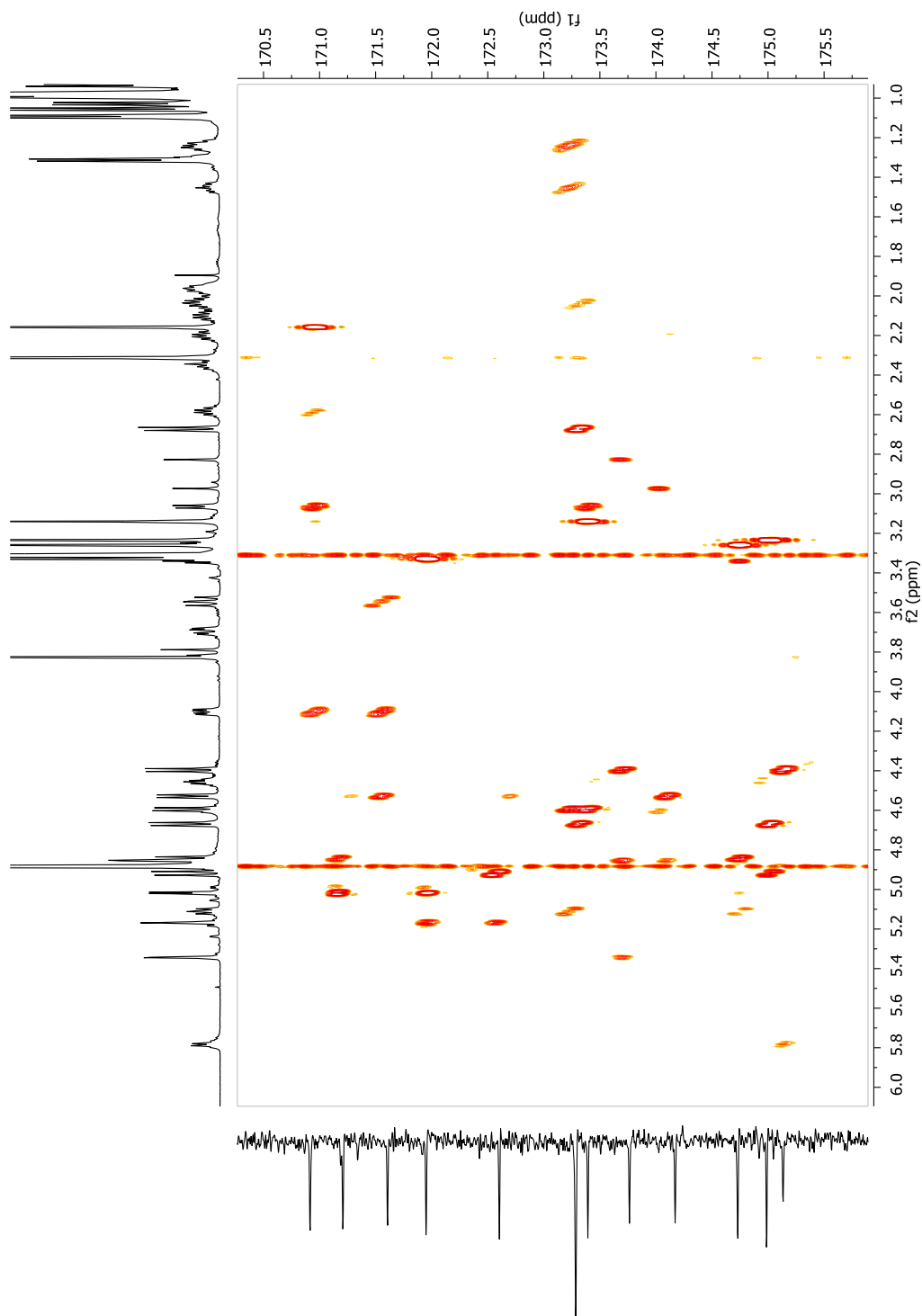


Figure S12. Semi-selective HMBC spectrum of **1** aliphatic methyl region, in CD₃OD (600 MHz, Bruker Avance 600). The spectrum was acquired at (TD) 4096x256, in 48 scans. It was zero filled to 4kx4k, with forward linear prediction on f1 direction.

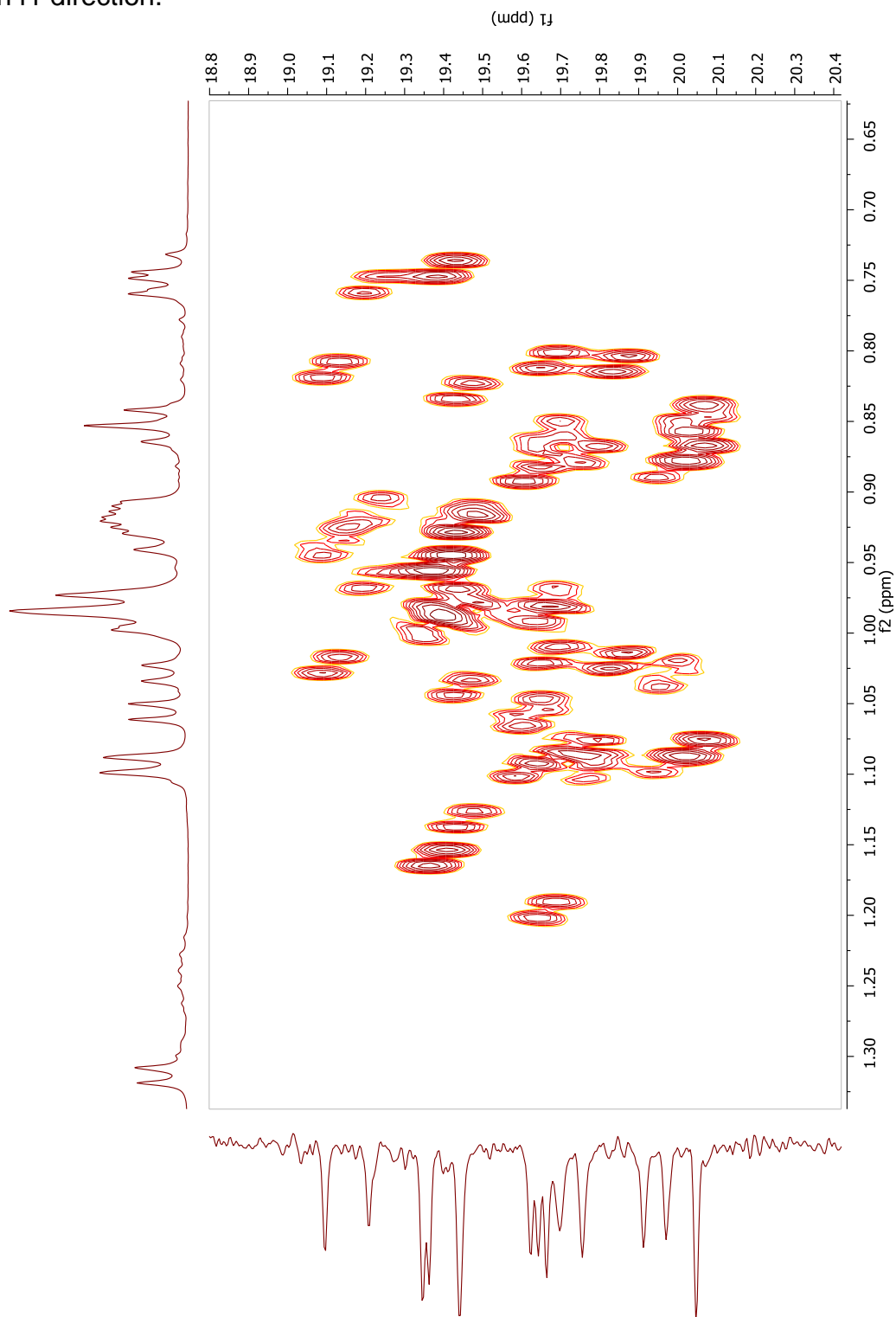


Figure S13. ROESY spectrum of **1** in CD₃OD (600 MHz, Bruker Avance 600). The spectrum was acquired at (TD) 2048x256, in 32 scans. It was zero filled to 4kx4k, without linear prediction. The spectrum was not symmetrized during processing.

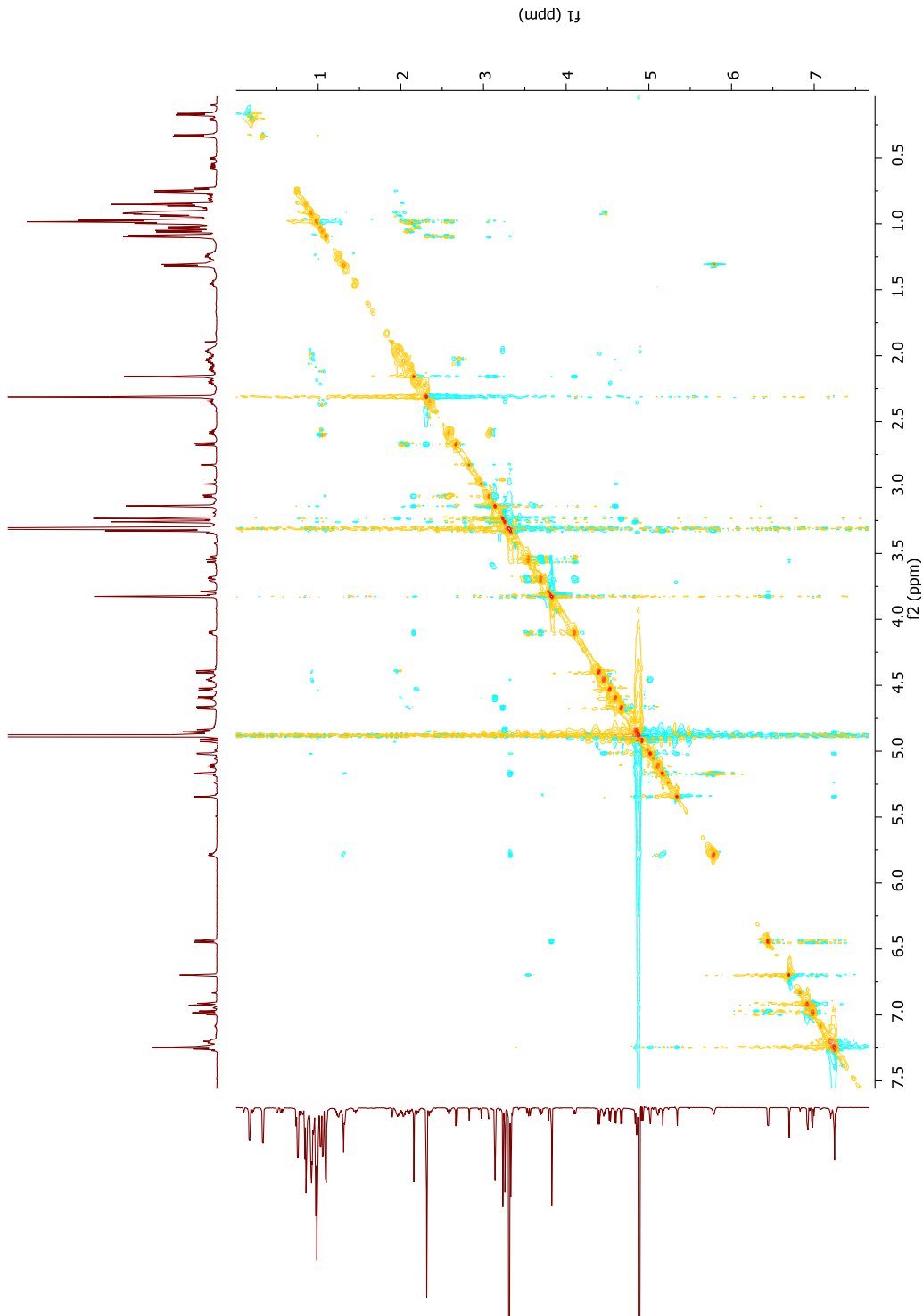
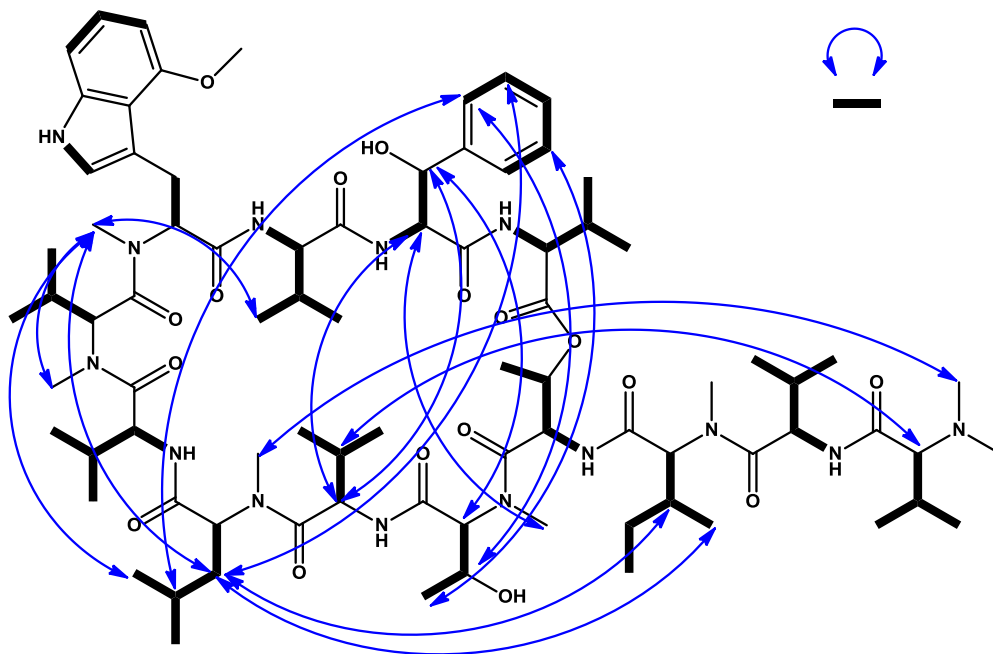


Figure S14. Observed ROESY correlations for **1**.

V. MS spectra and assignments.

Figure S15. LC-MS² spectrum of 1.

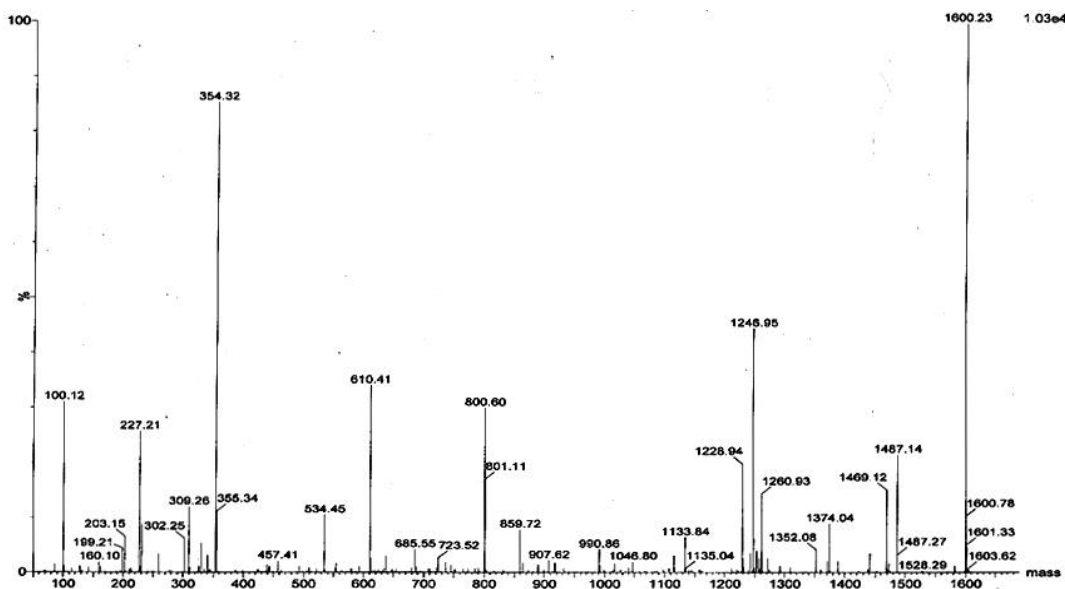


Figure S16. Fragmentation pattern in tandem mass spectroscopy provided conclusive evidence for the planar structure of 1.

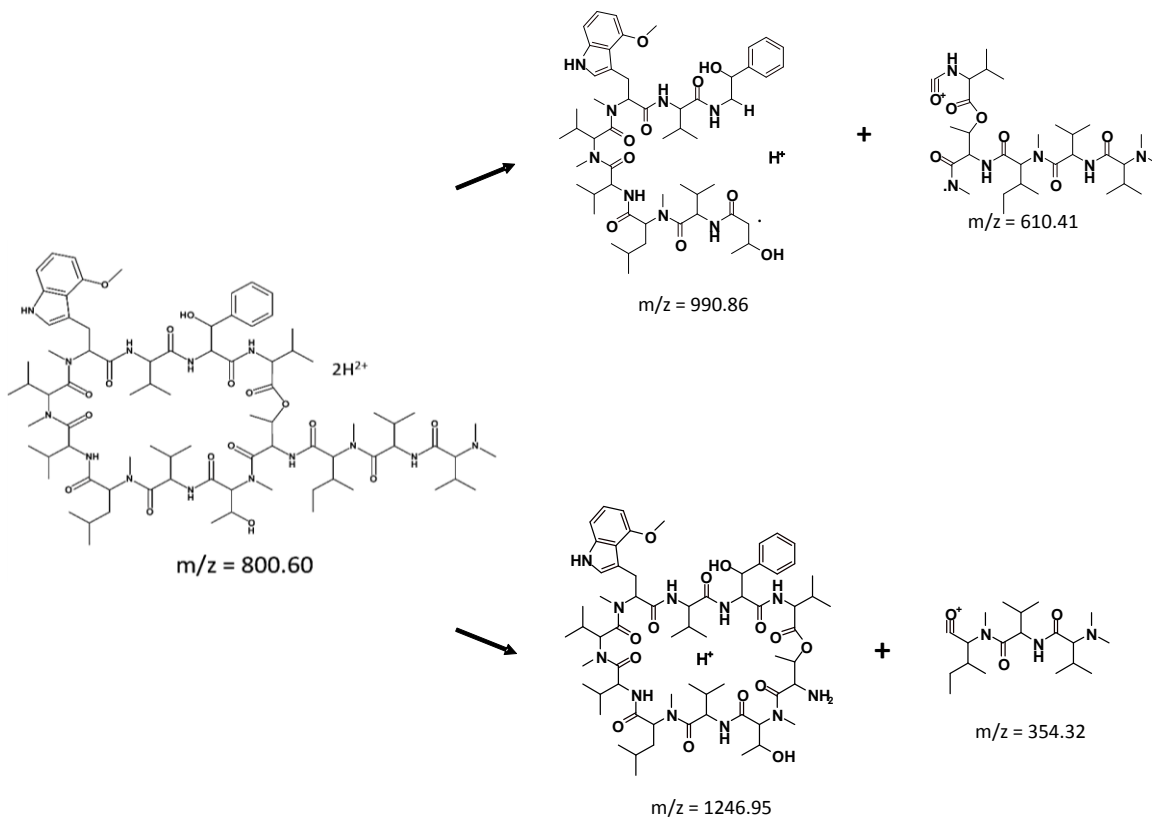
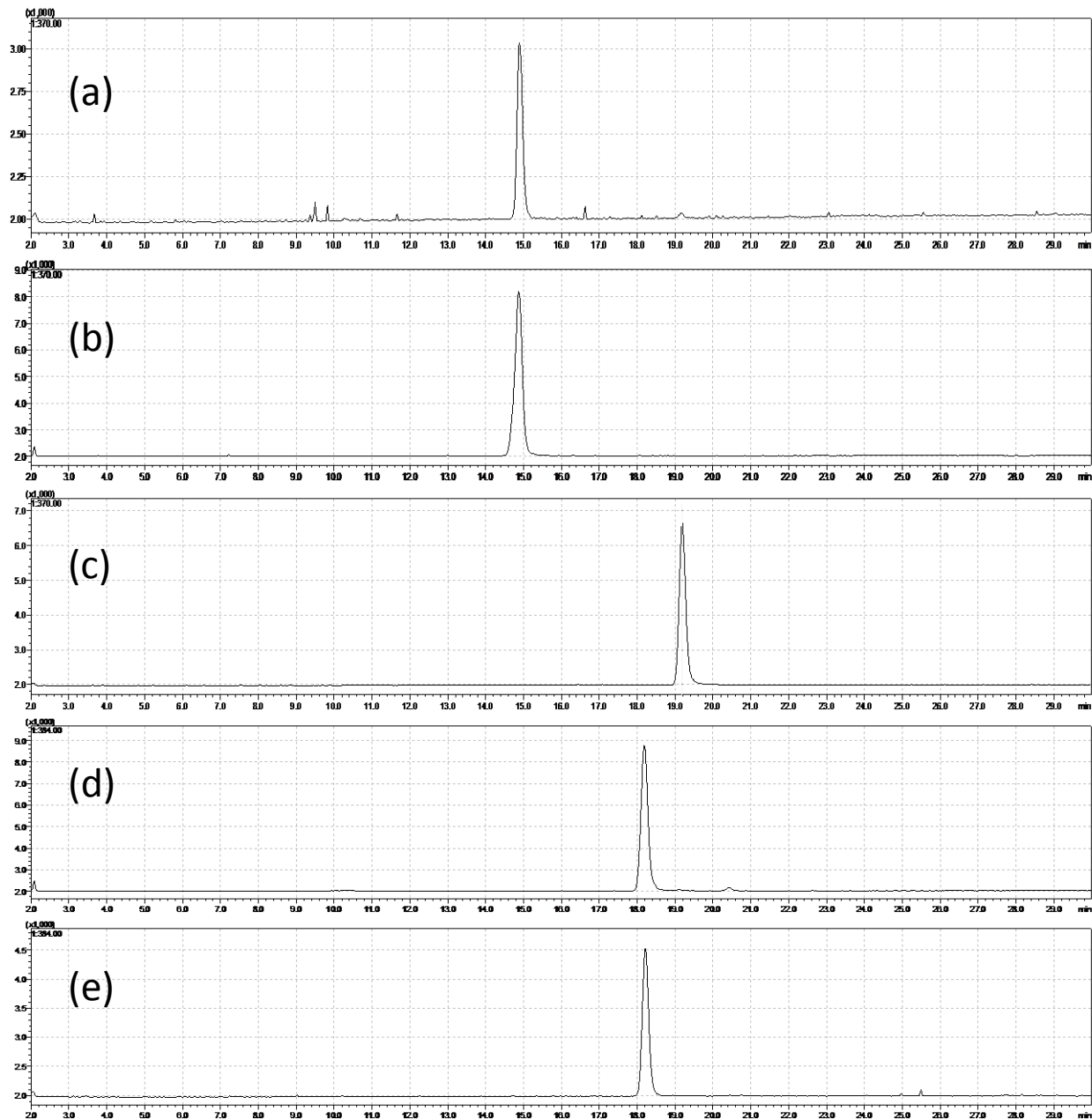


Figure S17. Result of the Marfey's experiment.

LC-ESI-MS (Shimadzu 2020) on a RP C18 column; peaks shown in (a), (b), and (c) were detected with SIM mode at $m/z = 370.3$; peaks shown in (d) and (e) were detected with SIM mode at $m/z = 384.0$.

(a) Hydrolate of **1** reacted with L-FDAA, r.t. = 14.87 min.

(b) L-ala-NH₂-DNP-L-valine, r.t. = 14.87 min.

(c) L-ala-NH₂-DNP-D-valine, r.t. = 19.19 min.

(d) Hydrolate of **1** reacted with L-FDAA, r.t. = 18.22 min.

(e) L-ala-NH₂-DNP-N-methyl-L-valine, r.t. = 18.22 min.

VI. X-ray crystallography data.

Figure S18. Oak Ridge Thermal-Ellipsoid Plot Program representation of the asymmetric unit of ecumicin, shown at 50% probability displacement ellipsoids. X-ray data were collected on a Bruker D8 discover X-ray system at room temperature and the crystal diffracted X-ray to 0.83 Å. Crystal data for ecumicin: $C_{83}H_{134}O_{17}N_{14}$, $M = 1599.01$, space group $P2_12_12$ (no. 18), $a = 71.64(7)$ Å, $b = 11.434(11)$ Å, $c = 12.697(13)$ Å, $V = 10400.110$ Å³, $Z = 4$, $F(000) = 3972$, $D_c = 1.172$ g/cm³, μ (MoK α) = 18.71 cm⁻¹, $T = 293(2)$, 1142 variables refined with 10140 reflections with $I > 4\sigma(I)$ to $R1 = 0.1722$. The structure was solved by direct methods using ShelxD program and refined by full-matrix least-squares using ShelxL.

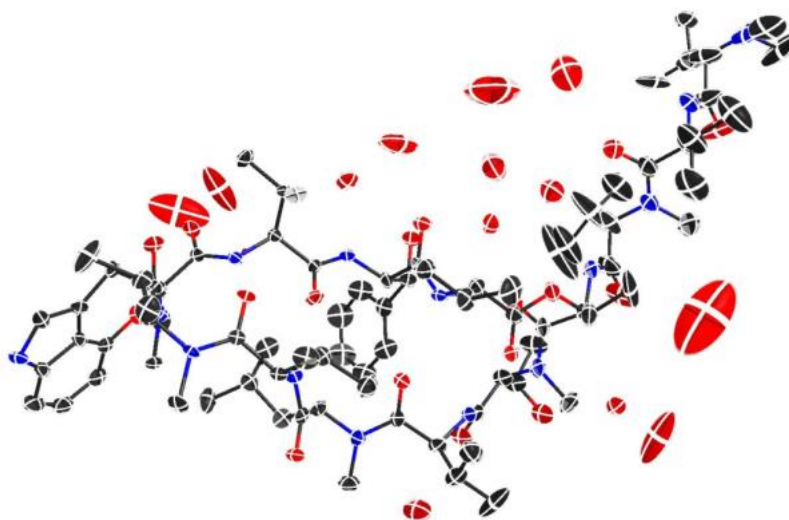


Figure S19. The *B*-factor putty tube representation of ecumicin shows that its structure is mostly ordered, with only the two *N*-terminal amino acids showing flexibility. The segments with the highest temperature factor are shown as thicker red cylinders.

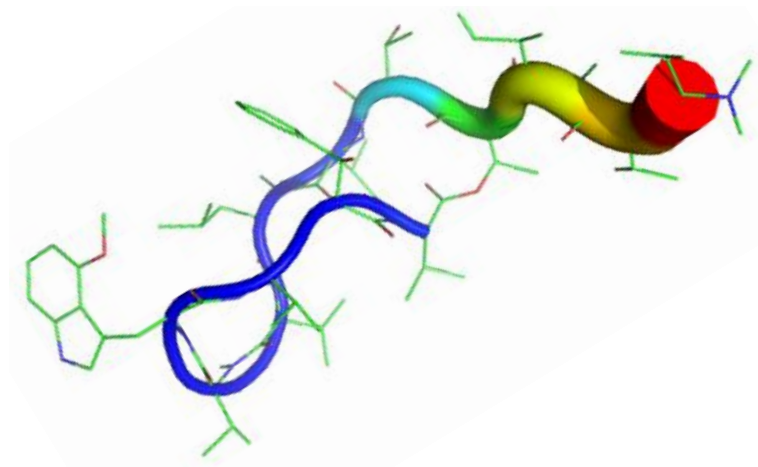


Table S1. Summary of carbonyl groups that may contribute to $n \rightarrow \pi^*$ interactions in ecumicin (AA = amino acid residue).

AA (C=O) ¹	AA C(=O) ²	$d_{n \rightarrow \pi^*}$ (Å)	θ
V ³	N-Me-V	2.647	97.6°
N-Me-V	N-Me-4-OMe-W	2.911	124.4°